AIAA JOURNAL
Vol. 38, No. 11, November 2000

Two-Color Planar Doppler Velocimetry

Stephen A. Arnette*
University of Dayton, Dayton, Ohio 45469
Gregory S. Elliott† and Andrew D. Mosedale‡
Rutgers University, Piscataway, New Jersey 08855
and
Campbell D. Carter§
U.S. Air Force Research Laboratory, Wright–Patterson Air Force Base, Ohio 45433

A novel two-color approach to planar Doppler velocimetry (PDV) is demonstrated in a supersonic flow. The technique was implemented using a frequency-doubled Nd:YAG laser and a Nd:YAG-pumped dye laser ($\lambda = 618$ nm) for illumination and a color charge-coupled device (CCD) camera for detection. In testing two-color PDV, we obtain good agreement between experimental and theoretical velocities (difference of $\sim 11\%$) in a compressible freejet flow. The two-color approach enjoys an inherent advantage over single-color systems in that both the filtered and reference flow images are captured with a single camera. The need to split the scattering (and direct to two cameras) is eliminated, and the fields of view of the filtered and reference images are naturally aligned. Thus, the difficulty of experimental setup, which is an impediment to the wide application of PDV, is significantly reduced. Furthermore, the needed equipment, at least for one velocity component, was essentially that employed for particle-imaging velocimetry (PIV). However, as a tradeoff one must characterize the irradiance distributions of the two laser sheets, as well as carefully overlap the two sheets within the probe region, and record the beam energies for the two lasers on a shot-by-shot basis. Furthermore, as seed particle size increases beyond the Rayleigh limit (where $d_{\text{Rayleigh}} < 100$ nm for visible wavelengths) the ratio of red and green scattering signals will depend on particle size. Nonetheless, the ease with which the two-color PDV technique can be applied, and its complementary nature with equipment needed for PIV, makes it attractive. The strengths and weaknesses of our particular approach are discussed, namely CCD color bleed effects, as are potential alternatives.

Introduction

THE potential value of a planar, instantaneous, nonintrusive velocimetry technique has spurred significant effort in applying atomic/molecular vapor filters to measure the Doppler shift contained in scattered light. Shimizu et al.[1,2] were the first to propose the use of an atomic vapor filter to eliminate aerosol scattering in LIDAR thermometry. Later, Meyers and Komine,[3] Komine et al.,[4] Meyers,[5] and Miles et al.[6,7] demonstrated the feasibility of employing molecular iodine (I_2) vapor filters for flow diagnostics. From this work, two very similar filter-based approaches have emerged that enable the measurement of planar velocity fields from particle scattering. The most significant difference is that in one approach a single-mode, continuous-wave (cw) laser, for example, an argon-ion laser, is employed to record the time-averaged flowfield velocity; in the other approach, a pulsed, injection-seeded laser, for example, a Q-switched Nd:YAG laser, is employed, enabling the acquisition of instantaneous velocity images. Note that the respective praticioners of these approaches have typically employed different names: Doppler global velocimetry for the cw-laser-based (time-averaged) approach vs planar Doppler velocimetry (PDV) for the pulsed-laser-based (time-resolved) approach. In this paper we will use simply PDV, as the fundamentals of both approaches are the same.

The time-resolved PDV technique has been employed successfully to make instantaneous velocity measurements in a variety of high-speed flows. Typically, these measurements have included only a single velocity component.[8–11] More recently multiple-component measurements have been reported.[12–14] Although time-resolved PDV has been developed primarily for its potential in supersonic flows, McKenzie has shown that it is applicable to low-speed flows as well.[15,16] Indeed, Beutner et al.,[17] Mosedale et al.,[18] and Mosedale[19] have applied PDV in a large-scale subsonic wind tunnel to characterize the flow over a simple delta wing, demonstrating that accuracy (for the frame-averaged measurements) within ~ 2 m/s is feasible.

Two approaches have been employed to obtain the filtered and reference images required in measuring the Doppler shift at each point in the flowfield. In the split-image approach, the scattering is split into two parts, with one being directed through the filter. The two scattering beams, filtered and reference, are then recombined onto the same charge-coupled device (CCD) array. Though convenient in terms of equipment usage, this approach is characterized by a tradeoff between speckle and image-overlap effects because the overlap is mitigated with a small lens aperture.[19] In the two-camera approach, two detectors are located side by side, with the atomic/molecular filter placed before one of the detectors. In either case, normalizing the filtered image by the reference image, which gives the Doppler shift when combined with the known absorption profile, requires an accurate alignment procedure. Although subpixel accuracy can be achieved in aligning the filtered and reference fields of view, maintaining this alignment may be more difficult in large-scale test facilities and during long-duration tests; this is true for both the two-camera and split-image approaches. In addition, in certain cases, placing an alignment target, for example, a dot card, at the object plane may not be feasible or at least convenient. One potential approach to simplifying the PDV technique is to use two laser wavelengths and a color CCD camera, as one does with the two-color particle imaging velocimetry (PIV) technique.[20] The results of a study of the feasibility of two-color PDV are reported here, including 1) validation of the two-color approach, 2) identification of some of the major challenges associated with the technique, and 3) acquisition of velocity images in supersonic jet flows. Note that in our implementation of two-color PDV, we employed a working two-color PIV system. Two colors are used for the

Received 17 April 1999; revision received 7 April 2000; accepted for publication 12 May 2000. Copyright © 2000 by the authors. Published by the American Institute of Aeronautics and Astronautics, Inc., with permission.

*Assistant Professor, Department of Mechanical Engineering; currently Vice President, Sverdrup Technology, Inc., Tullahoma, TN 37388. Member AIAA.

†Assistant Professor, Department of Mechanical and Aerospace Engineering. Member AIAA.

‡Graduate student, Department of Mechanical and Aerospace Engineering; currently Engineer, Adaptco, Melville, NY 11747.

§Research Scientist, Innovative Scientific Solutions, Inc., Dayton, OH 45440. Associate Fellow AIAA.

PIV so that directional ambiguity can be resolved and cross correlations (rather than autocorrelations) can be employed to determine the particle displacement. In this study we sought to answer the following question: through modest changes, principally addition of the I_2 cell before the camera, could one convert a PIV system to a PDV system? Of course, one potential problem is that at any particular viewing angle, the scattering intensity can be a strong function of wavelength as the particle size increases beyond the Rayleigh limit. This issue, along with others, is discussed in detail hereafter.

Experimental Procedure

A schematic of the setup for the experiments is shown in Fig. 1. Two supersonic freejets were employed in this study. In both, the air issued vertically through a converging–diverging nozzle (12.7-mm exit diameter) designed using the method of characteristics. The design Mach number of the first nozzle was 1.5 and that of the second was 1.36. For experiments with the Mach 1.5 nozzle, water-condensation particles were formed when moist ambient air was entrained into the mixing layer surrounding the jet; these particles were used as the scattering medium. Accordingly, the flow was imaged, and the velocity was derived, only at those points where the local mixedness was sufficient for condensation particles to be formed. For experiments with the Mach 1.36 nozzle, ethanol was injected into the stagnation chamber, and the resulting condensation particles served as the scattering medium. Both cases are less than ideal in that the entire field; that is, jet flow and surrounding ambient fluid, is not seeded, but this was not required to achieve the primary objective: an assessment of the feasibility of two-color PDV. Note that there have been several estimates of particle size associated with condensation seed (see Ref. 12, for example); however, these estimates have typically been based solely on the observation that the scattering characteristics are consistent with the Rayleigh scattering regime.

The 100-mJ/pulse red beam from a Lumonics Hyper-Dye dye laser (0.1 cm^{-1} linewidth, pumped by a Nd:YAG laser) and the 100-mJ/pulse green beam from an injection-seeded Nd:YAG laser (Quanta-Ray GCR-150) were combined using a dielectric mirror and formed into sheets using a negative cylindrical lens followed by a positive spherical lens; for both, the polarization vector was within the sheet. The sheets were carefully overlapped and focused in the probe region; a simple two-lens telescope was employed with the red beam to ensure that its focal position matched that of the green beam. The camera axis was oriented at 29.5 deg above the nozzle exit plane (60.5 deg from the jet axis) for the Mach 1.5 jet and parallel to the nozzle exit plane (90 deg from the jet axis) for the Mach 1.36 jet. Neglecting the small divergence of the sheets, the propagation direction was perpendicular to the jet centerline for the Mach 1.5 jet experiments and 10 deg off the jet axis for the Mach 1.36 experiments. The pulse duration of each laser, ~10 ns, is sufficiently short to yield effectively instantaneous velocity measurements. The

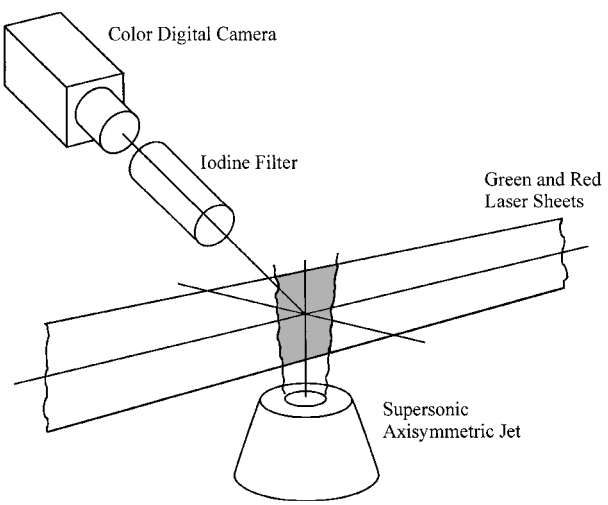

Fig. 1 Schematic of the configuration for experiments with the Mach 1.5 jet.

timing of the two lasers was controlled with a Stanford Research Systems digital delay generator, and the arrival of the laser pulses in the probe volume was synchronized to within ~10 ns. Note that although two Nd:YAG lasers were employed (again, the lasers and optics were configured for PIV), two are not required: one injection-seeded Nd:YAG could be used to provide the resonant green beam and to pump a dye laser.

A Kodak DCS 460 color CCD camera, having 3060 × 2036 pixels (each 9 μm square), had been used for the PIV measurements and was thus used here. This camera is intended for photographic rather than scientific applications; the CCD is housed in a Nikon N3 camera body and includes the standard mechanical shutter (with useable laser-synchronized shuttering times as small as ~12 ms). The camera was fitted with a Micro-Nikkor 105-mm f/2.8 lens that was operated at maximum aperture to mitigate speckle. Speckle noise is introduced when coherent electromagnetic radiation is scattered from a surface or ensemble of particles; small differences in path length (from scatterers to the detector) result in the formation of a three-dimensional interference pattern. Smith[21] and McKenzie[16] have shown that speckle noise is proportional to the lens f-number and inversely proportional to the average dimension of the detector resolution element. Thus, small pixels are not ideal where speckle noise is concerned; however, the large number of pixels of each color allows speckle to be mitigated through pixel binning, which effectively increases the average resolution element dimension.

Although the Kodak DCS 460 detector offers 12-bits/color, the device driver employed to acquire images into the Adobe Photoshop™ software package was only an 8-bit driver; a 12-bit driver is currently available, but detector read noise may limit the dynamic range. The color mask employed by the camera includes alternating rows of red–green and green–blue filters; thus, green pixels account for one-half of the total, whereas the red pixels account for one-quarter of the total pixels. Note that the green filter transmits red light, and, thus, color bleed must be characterized to obtain accurate velocity measurements. On the other hand, the red filter does not transmit a significant portion of the green light, according to Kodak's specifications.

To track and control the laser frequency, we implemented a wavelength reference system, or wave meter, consisting of a reference I_2 cell, fast photodiodes, and Stanford Research Systems gated integrators and computer interface.[18,19] This wave meter also included a station (complete with a third photodiode and gated integrator) for the camera I_2 cell, to permit simultaneous calibration with the reference I_2 cell. With the wave meter, we monitored the laser for drift of its set-point frequency but did not record the frequency with each velocity image. The shot-to-shot frequency variations, about ±10 MHz, are small, however, relative to the Doppler shift. The 7.6-cm-diam, 20-cm-long Pyrex cell body was wrapped with heat tape and maintained at 378 K (Ref. 19). The I_2 partial pressure was controlled by circulating water (from a temperature-controlled bath) through a jacket surrounding an I_2 reservoir with temperature set at 313 K. Also, for the purpose of broadening the transition, 20 Torr partial pressure of N_2 was added to the cell.[18] Note that we employed slightly different cell conditions for measurements in the Mach 1.5 jet.

Results and Discussion

To determine velocity the measured transmission must be converted to the Doppler frequency shift $\Delta\nu$ using the I_2-filter frequency-transmission relationship. The scatterer's velocity vector $\boldsymbol{V}$ is related to $\Delta\nu$ by

$$\Delta\nu = \nu_s - \nu_0 = (\nu_0/c)(\boldsymbol{k}_s - \boldsymbol{k}_0)\cdot\boldsymbol{V} \tag{1}$$

Here, $\boldsymbol{k}_s$ and $\boldsymbol{k}_0$ are the respective observed (scattered) and incident unit light-wave propagation vectors, c is the speed of light, and ν_s and ν_0 are the respective frequencies of the scattered and incident (laser) radiation. By the use of this relationship, the velocity of a particle can be found if the Doppler shift of the scattering can be determined. This is accomplished by measuring the transmission of the frequency-doubled Nd:YAG scattering through the I_2 filter and comparing this to the independently measured absorption profile.

Relative to past PDV systems, the two-color approach employed here is simply an alternative means of determining the transmission through the filter. The camera records green and red particle scattering images through the I_2 filter. The green scattering is attenuated by an amount that is dependent on the Doppler shift present in the scattering. The red scattering is attenuated as it passes through the filter, but the attenuation is not frequency dependent (primarily reflective losses). Determining the transmission of the green light at each pixel in the image requires a measurement of the unfiltered green scattering field. By acquiring images with the filter in place, the relationship between recorded green and red counts at each point in the array can be established. With this relationship, the desired green transmission, $I_{grn}/I_{grn,0}$, is given by

$$\frac{I_{grn}}{I_{grn,0}} = \frac{I_{grn}}{(I_{grn,0}/I_{red})I_{red}} = \frac{I_{grn}}{(I_{grn,0}/I_{red,0})(I_{red,0}/I_{red})I_{red}} \quad (2)$$

where I_{grn} and I_{red} are the respective green and red intensities recorded through the filter and $I_{grn,0}$ and $I_{red,0}$ are the respective green and red intensities that would have been recorded without the filter. The ratio $[I_{grn,0}/I_{red,0}]$ was determined in situ from flow images acquired without the filter in place, while $[I_{red,0}/I_{red}]$ was determined by simply measuring the transmission of the red beam through the filter. In this way, instantaneous filter-transmission ratios for the green scattering can be acquired without image splitting and subsequent recombining. This is the defining characteristic of the two-color approach to molecular-filter velocimetry. Of course, establishing the correct relationship between red and green pixels requires, at the very least, shot-to-shot energy measurements for red and green beams. However, the variations of the shot-to-shot energies were relatively small, ±0.8% for the green beam and ±3.5% for the red (dye laser) beam; thus, no attempt was made to correct the derived velocity images for this variation, and, indeed, no mechanism to do this was readily available. It will be seen later, however, how this variation can lead to noise in the velocity image. Likewise, variation in the irradiance distribution of the dye laser sheet can also lead to measurement error.

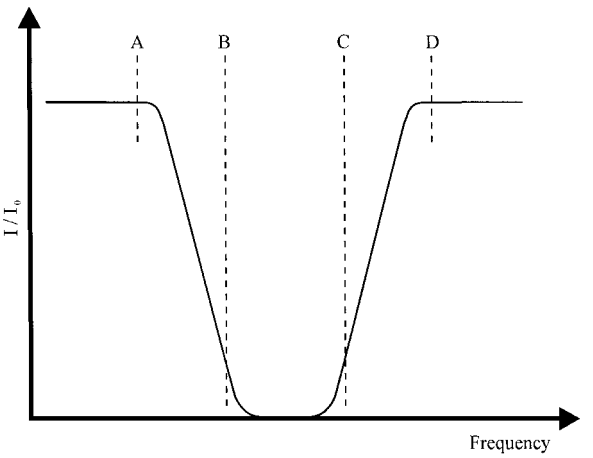

Fig. 2 Schematic of the I_2-filter absorption profile; frequency set points labeled A–D correspond to images in Fig. 3.

In our experiment, the seed particles are generated from condensation of water or ethanol and are sufficiently small to be described as Rayleigh scatterers. However, a general limitation of using two colors is that I_{grn}/I_{red} will be sensitive to particle size as the particle size increases beyond the Rayleigh limit[22–24]; indeed, particle sizing can be accomplished through the characterization of the I_{grn}/I_{red} function vs viewing angle (see Ref. 22, pp. 396–401). To study this problem, we solved the Mie scattering equations within the software package Mathcad™. From Mie theory, which describes scattering from spherical, homogeneous dielectric particles, one finds that the scattering intensity can be increasingly sensitive to the particle diameter d (as well as viewing angle) as the nondimensional particle size $\pi d/\lambda$ approaches unity. That is, the polar scattering intensity distribution will have lobes, the number of which will scale with $\pi d/\lambda$. In the neighborhood of these lobes, the ratio of maximum to minimum scattering intensity can be very large (a variation of an order of magnitude or more is possible). Thus, I_{grn}/I_{red} will be sensitive to d because either I_{grn} or I_{red} may be near a minimum, depending on d. As a practical guide for minimal sensitivity of I_{grn}/I_{red} to particle size, the particle diameter should not exceed ~100 nm for a moderate refractive index, for example, $n \leq 1.5$ (because a further constraint for Rayleigh scattering is that $n\pi d/\lambda$ also be small). Of course, the collection of seed particles may deviate significantly from a monodisperse distribution of spherical, homogeneous particles, and, thus, the exact dependence of scattering intensity on viewing angle and mean particle size may be difficult to predict a priori. (The scattering may not be described by Mie theory.) Nonetheless, caution should be exercised in applying the two-color approach with seed particles that cannot be approximated as Rayleigh scatterers because I_{grn}/I_{red} will be sensitive to the mean particle size: variation in the mean particle size in time and/or space can translate into errors in the velocity determination.

To assess the efficacy of the two-color approach with Rayleigh scatterers, we employed the Mach 1.5 jet and recorded scattering images at various laser frequencies (denoted A–D in Fig. 2) near the isolated I_2 transition at $\nu_0 = 18{,}789.3\ \text{cm}^{-1}$. The corresponding scattering images, shown in Figs. 3a–3d, have been cropped from the full array to about 650 × 1100 pixels. The flow direction is from right to left, and the illuminated portion of the jet extends from $x =$ 120 to 155 mm ($x/D = 9.45$–12.25).

In Fig. 3a (set point A in Fig. 2), scattering from the higher velocity regions of the jet is Doppler shifted into the absorption well

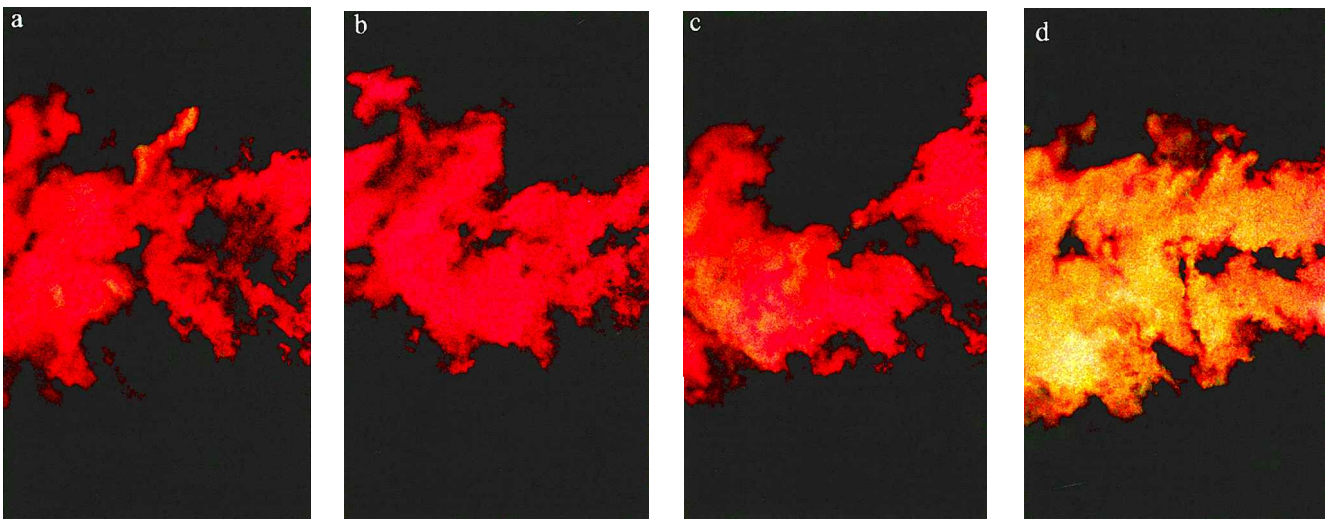

Fig. 3 Instantaneous (uncorrelated) color PDV images from a Mach-1.5 freejet; each image (3a–3d) corresponds to a laser-frequency set point shown in Fig. 2, A–D; flow is from left to right.

of the I_2 filter. As a result, most of the green scattering from the central region of the jet is absorbed by the filter, giving the image a predominantly red appearance. In the outer portions of the jet where the flow velocity is lower due to mixing with entrained ambient fluid, the Doppler shift is less severe. Significant green signal is present at these locations, and the green and red scattering combine to produce a yellow scattering image. For the laser frequency employed for Fig. 3b (set point B, Fig. 2), essentially all Doppler-shifted green scattering is absorbed by the filter, with only red scattering remaining. For the laser frequency of Fig. 3c (set point C, Fig. 2), the transmission increases with flow velocity. Accordingly, the central portions of the jet become more yellow and the outer portions predominantly red. For Fig. 3d (set point D, Fig. 2), the laser frequency and scattering are outside the absorption well, and the entire imaged region appears yellow. These images demonstrate the feasibility of the two-color approach for molecular-filter velocimetry and were used to choose the laser frequency for quantitative measurements. Furthermore, these images highlight a novel aspect of two-color PDV: the combination of colors gives the experimenter immediate feedback on the distribution of velocities in the flowfield.

The composition of a single instantaneous velocity measurement is presented in Fig. 4. The original filtered image is presented as Fig. 4a, and the extracted red and green images are presented in Figs. 4b and 4c, respectively. The instantaneous velocity image is presented in Fig. 4d, along with the corresponding gray scale relating intensity to velocity; note that in processing the images, we eliminated from consideration those pixels with red signal below a threshold value, thereby discriminating against poorly seeded regions. Furthermore, in determining the velocity, it was assumed that the Doppler shift was due to streamwise velocity only, that is, no circumferential velocity components were present in the jet. Because the jet is highly turbulent, this assumption is marginal for the instantaneous image, although the streamwise velocity would be much larger than the cross-stream components, but reasonable for the average velocity field. The streamwise jet velocity obtained from isentropic theory is 433 m/s, resulting from stagnation pressure and temperature of 372 kPa and 295 K, respectively; this corresponds favorably to the velocity magnitudes in Fig. 4d. As noted earlier, the color distribution is a good qualitative indicator of the distribution of velocities; this is evident in comparing the raw acquisition image Fig. 4a to the processed velocity image Fig. 4d.

Kodak employs a proprietary interpolation scheme to generate full, three-color images from the interlaced array, which is a concern in considering this camera for use in two-color PDV. An algorithm developed for the purpose of processing PIV data was employed to separate the Kodak composite image into its true-red and true-green component images. The single-color illumination data were processed with this algorithm before examining the data for bleed effects. By passing either the red or the green beam through a diffusing optic onto a screen and acquiring images with the color detector, the performance of the detector with respect to color bleed (red signal onto interpolated green channel or green signal onto interpolated red channel) could be investigated. Absorptive neutral-density filters were inserted in the beam path, permitting variable attenuation of the incident beam.

The effect of bleed is illustrated in Fig. 5, where the average ratio of green to red signal counts with red-only ($\lambda = 618$ nm) illumination of a diffuse surface is shown. As indicated in Fig. 5, the resulting green readings are ~36% of the corresponding red values over the range of red intensities incident on the array. Note that signal levels less than ~10 counts are significantly influenced by the background light. Also shown in Fig. 5 is the ratio I_{grn}/I_{red} after accounting for the bleed (shown with the triangles); that is, 35.8% of the red reading was subtracted from the green reading at the same pixel. The resulting corrected green readings are close to but slightly above zero because the correction resulted in negative green levels, and these were entered into the data array as zeros, biasing the average to finite positive levels. Note that this problem would not be encountered in practice given the use of two-color illumination. Surprisingly, with green-only illumination, the signal levels of the red pixels were about 9.6% of those of the corresponding green pixels. The higher-than-expected green-to-red bleed probably reflects the performance of our algorithm in extracting true colors rather than an error in Kodak's filter specifications.

The spatial variation in the irradiance profiles of the green and red beams was also investigated. As might be expected, the dye laser's irradiance profile exhibited somewhat more temporal variation than that of the Nd:YAG laser. Of course, this is important because the technique depends on a known (preferably constant) ratio of the green and red irradiance profiles. While a dye laser was readily available for this experiment, it may not be the best choice for the nonresonant illumination, insofar as its spatial irradiance

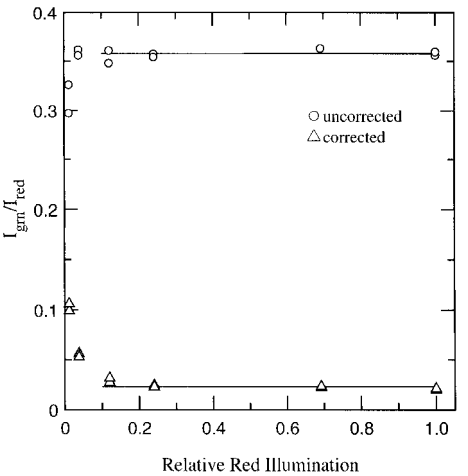

Fig. 5 Ratio of green and red pixel readings as a function of red (only) illumination before (○) and after (△) bleed correction.

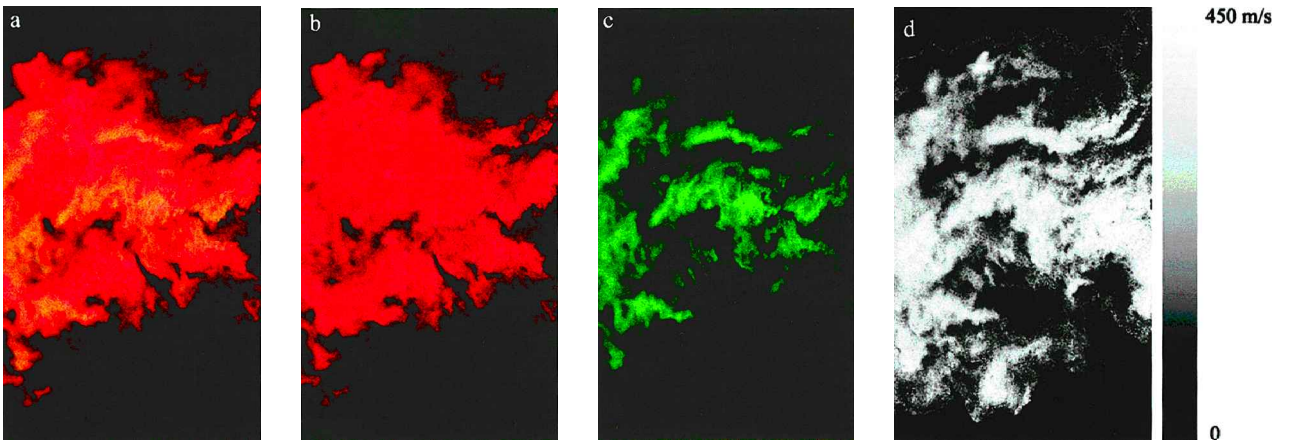

Fig. 4 Composition of a two-color PDV image: a) two-color image, b) extracted red image, c) extracted green image, and d) resulting gray scale velocity image (with velocity scale shown on the right).

profile is subject to greater variation than that of a solid-state laser. However, dye lasers, especially of the broadband design, are easily set up, and the increase in spectral bandwidth ($\sim 150\ \mathrm{cm}^{-1}$ with Exciton Rhodamine 640) would ameliorate speckle noise. Along these lines, one might also use a so-called modeless dye laser, which employs amplified spontaneous emission (ASE) rather than stimulated emission; again, the goal would be speckle mitigation through minimization of the coherence length. Finally, we note that experiments utilizing the red beam from a Nd:YAG-pumped N_2-Raman cell ($\lambda = 607$ nm) were also attempted; here, variations in the shot-to-shot beam energy and irradiance distribution exiting the Raman cell were large, and no further efforts were made to implement the Nd:YAG-pumped Raman cell in the two-color experiments.

Although the DCS 460 camera was suitable for demonstrating the feasibility of the two-color technique, a CCD that minimizes bleed effects while also exhibiting a good detection limit would improve the performance of the two-color approach. These two conditions may be more easily met with the three-chip-type (one-chip/color) cameras; here, however, the image-splitting optics may be polarization sensitive (i.e., the splitting ratio depends on input polarization) and/or impose f-number limitations. Alternatively, in lower-speed flows, one might employ an interline-transfer camera to obtain two images, filtered and reference, on the same CCD chip. For example, with the Princeton Instruments MicroMax camera (model 1300YHS-DIF), which can also be used for PIV, one can obtain consecutive exposures (by shifting the charge in each row to an adjacent charge-storage row) with time separations as small as 200 ns. A microlens array employed by this CCD camera improves the fill factor, to $\sim 60\%$, but also limits somewhat the f-number (both of which affect the speckle noise). Nonetheless, with an interline-transfer camera, the wavelength of the reference laser could be any value detectable by the CCD chip; indeed a second injection-seeded laser, with wavelength tuned outside the I_2 absorption line, could be used. Of course, using two injection-seeded Nd:YAG lasers, or deriving two single-mode pulses of different cavity order (separated by ~ 500 MHz in frequency and 200 ns in time, for example) from a single laser, would effectively eliminate Mie-scattering particle-size concerns. In the latter case, sheet overlap errors would also be eliminated, although velocity errors could still arise from the finite time separation between filtered and reference images.

Quantitative instantaneous and average velocity images (based on 20 samples) incorporating the intensity-correction procedure are presented in Fig. 6. Here, the viewing angle was normal to the plane of the illuminating sheet. The illuminating sheet contained the centerline of the jet (flow propagation axis), and the direction of propagation of the laser light was 10 deg with respect to the jet centerline. This geometry results in the following vector values: direction of collection equals $\boldsymbol{i}$ and laser propagation direction equals $0.174\boldsymbol{j} - 0.985\boldsymbol{k}$. The flow direction is from bottom to top, and the streamwise extent of the images is from $x = 32$ to 117 mm ($x/D = 2.5$ to 9.25). The stagnation conditions, pressure and temperature of 283 kPa and 295 K, respectively, for the perfectly expanded jet correspond to a theoretical axial exit velocity of 403 m/s. The derived average velocity within the jet core (near the jet exit) is 446 m/s, after accounting for the angle $\boldsymbol{k}_s - \boldsymbol{k}_0$, and this represents a deviation of 10.7% from the theoretical value. To avoid any bias in the calculation of the average image, only those pixels with signal levels above a threshold value and below the saturation value were included in the calculation of the average image; this required that we track the number of valid frames for each pixel. Pockets of high-velocity gas near the bottom of the average image suggest that the jet was actually slightly underexpanded, which would give rise to a somewhat higher velocity than the theoretical value. The results for a strongly underexpanded jet (stagnation pressure of 387 kPa) with the same nozzle are presented in Fig. 7. The resulting shock cell structure is clearly evident in the velocity images. The average within the core (near the jet exit) is 500 m/s, a larger velocity relative to the perfectly expanded case, as expected.

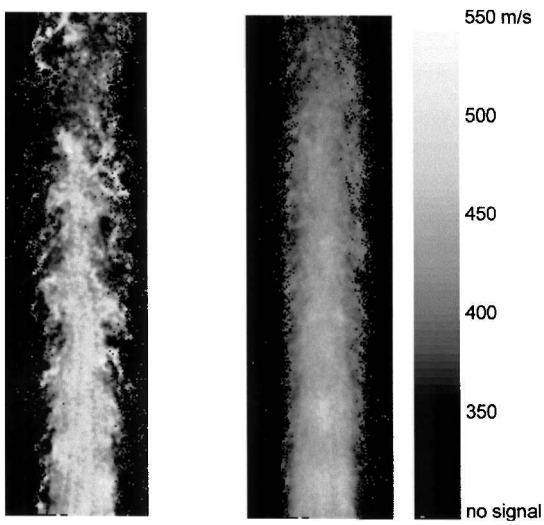

Fig. 6 Two-color PDV results for the velocity in a perfectly expanded Mach 1.36 freejet; left- and right-hand images show one of the instantaneous and the frame-averaged velocities, respectively; derived mean velocity within the jet core is 446 m/s.

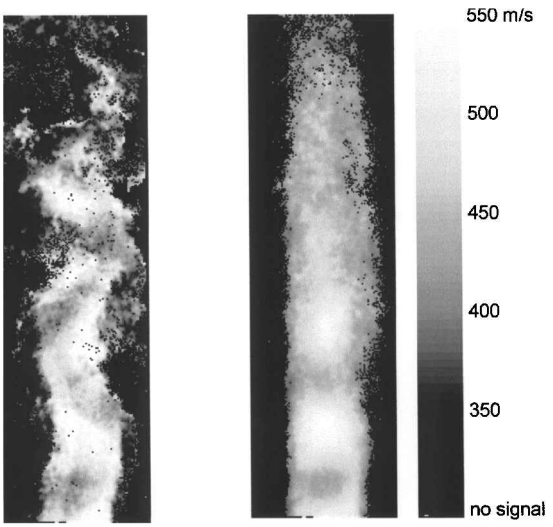

Fig. 7 Two-color PDV results for the velocity in an underexpanded Mach 1.36 freejet; left- and right-hand images show one of instantaneous and the frame-averaged velocities, respectively; derived mean velocity within the jet core is 500 m/s.

In the core of the perfectly expanded jet, where the turbulence intensity is expected to be low, the rms of the velocities was found to be $\pm 7\%$ of the mean value (without image smoothing). Of course, this level of fluctuation is higher than would be expected for the core region; indeed laser Doppler velocimetry measurements showed that within the core of the jet (near the jet exit), time-dependent velocity fluctuations are no more than about $\pm 1\%$ of the mean. Instead, the PDV-derived value of 7% represents an instrumental precision that is a combination of speckle noise and normalization error, the latter apparently caused by shot-to-shot beam energy variations (relative to the mean calibration measurement). The normalization error is evident from the seeding nonuniformity in the scattering image propagating to the velocity image (see the vertical streaks in the instantaneous velocity image of Fig. 6), rather than being removed by ratioing the green and red images. Ideally, we would have recorded red and green beam energies with each image. With this information, we could have removed this source of noise, presumably reaching the 2–3% noise level with the addition of image smoothing. Of course, even with ideal normalization (limited only by shot noise) reaching the 1% noise level is made difficult by speckle.

Finally, note that during postprocessing no allowance was made for any variation in frequency across the beam profile. Some researchers, notably Forkey,[25] Forkey et al.,[26] and Clancy and Samimy[13] have reported a significant variation across the beam profile; for example, Ref. 25 reports a 100-MHz variation. Although no attempt was made here to characterize the variation for this laser,

only the central portion of the beam was employed, as suggested by Clancy and Samimy.[13]

Conclusions

A novel approach to PDV predicated on two-color illumination and color detection has been demonstrated in a supersonic flow. In applying this technique to a compressible freejet, we obtained good agreement (a difference of ~11%) between the experimental and theoretical velocities, thus validating the two-color concept. The two-color approach enjoys the advantage over single-color systems in that both filtered and reference flow images are captured with a single camera, eliminating the need to split the scattering. Concerns over accurate matching of filtered and reference fields of view, or maintaining this alignment, are obviated. This makes implementation of PDV only slightly more complicated than implementation of PIV, and, in fact, the same lasers and digital cameras (i.e., color or interline-transfer CCDs) can in principle be used for both velocimetry techniques. However, as a tradeoff, one must characterize the irradiance distributions of the two laser sheets, which can readily be done in situ, and record the energies for the two laser beams on a shot-to-shot basis. Also, for particles beyond the Rayleigh limit, $d_{\text{Rayleigh}} < 100$ nm for visible wavelengths and a moderate scatterer refractive index, the scattering intensity, and, thus, the ratio of the intensities of the two colors, will depend on the particle size. Nonetheless, with the ethanol/water condensation seed employed in this study (with particles satisfying the Rayleigh criterion), this approach was effective. Improvements would be realized by using a nonresonant laser with a more stable irradiance profile than obtainable with the dye laser. In addition, the technique would be improved with a digital camera with minimal color bleed and an improved detection limit. Other approaches and variations on our approach should be investigated with the goal of reducing the complexity of PDV and, thus, making the technique more useable.

Acknowledgments

This work was performed within the Propulsion and High-Speed Systems Branch of the Propulsion Directorate at Wright–Patterson Air Force Base, Air Force Research Laboratory (AFRL/PRSC). S. A. Arnette was supported by the Air Force Office of Scientific Research (AFOSR) (Grant F49620-97-1-0147), G. S. Elliott was supported under the AFRL Summer Faculty Research Program, and C. D. Carter was supported by the AFOSR (Grant F33615-97-C-2702). The authors are also indebted to J. M. Donbar (AFRL/PRSC) and J. Hoffman for their assistance with the experiments and to L. P. Goss and W. L. Weaver (Innovative Scientific Solutions, Inc.) for discussions regarding the use of the Kodak charge-coupled device camera.

References

[1]Shimizu, H., Lee, S. A., and She, C. Y., "High Spectral Resolution LIDAR System with Atomic Blocking Filters for Measuring Atmospheric Parameters," *Applied Optics*, Vol. 22, No. 9, 1983, pp. 1373–1381.

[2]Shimizu, H., Noguchi, K., and She, C. Y., "Atmospheric Temperature Measurements by High Spectral Resolution LIDAR," *Applied Optics*, Vol. 25, No. 9, 1986, pp. 1460–1466.

[3]Meyers, J. F., and Komine, H., "Doppler Global Velocimetry: A New Way to Look at Velocity," *Laser Anemometry*, Vol. 1, 1991, pp. 289–296.

[4]Komine, H., Brosnan, S. J., Litton, A. B., and Stappaerts, E. A., "Real-Time, Doppler Global Velocimetry," AIAA Paper 91-0337, Jan. 1991.

[5]Meyers, J. F., "Doppler Global Velocimetry: The Next Generation?" AIAA Paper 92-3897, July 1992.

[6]Miles, R. B., Lempert, W. R., and Forkey, J., "Instantaneous Velocity Fields and Background Suppression by Filtered Rayleigh Scattering," AIAA Paper 91-0357, Jan. 1991.

[7]Miles, R. B., Forkey, J., and Lempert, W. R., "Filtered Rayleigh Scattering Measurements in Supersonic/Hypersonic Facilities," AIAA Paper 92-3894, July 1992.

[8]Clancy, P., Elliott, G. S., Samimy, M., and Arnette, S. A., "Molecular Filter-Based Diagnostics in High-Speed Flows," AIAA Paper 93-0512, Jan. 1993.

[9]Elliott, G. S., Samimy, M., and Arnette, S. A., "A Molecular Filter Based Velocimetry Technique for High Speed Flows," *Experiments in Fluids*, Vol. 18, Nos. 1–2, 1994, pp. 107–118.

[10]Smith, M. W., and Northam, G. B., "Application of Absorption Filter-Planar Doppler Velocimetry to Sonic and Supersonic Jets," AIAA Paper 95-0299, Jan. 1995.

[11]Elliott, G. S., Mosedale, A., Gruber, M. R., Nejad, A. S., and Carter, C. D., "The Study of a Transverse Jet in a Supersonic Cross Flow Using Molecular Filtered Based Diagnostics," AIAA Paper 97-2999, July 1997.

[12]Arnette, S. A., Samimy, M., and Elliott, G. S., "Two-Component Filtered Planar Velocimetry in the Compressive Turbulent Boundary Layer," *Experiments in Fluids*, Vol. 24, No. 4, 1998, pp. 323–332.

[13]Clancy, P., and Samimy, M., "Multiple-Component Velocimetry in High-Speed Flows Using Planar Doppler Velocimetry," *AIAA Journal*, Vol. 35, No. 11, 1997, pp. 1729–1738.

[14]Clancy, P., and Samimy, M., "Planar Doppler Velocimetry: Three-Component Velocimetry in Supersonic Jets," AIAA Paper 98-0506, Jan. 1998.

[15]McKenzie, R. L., "Measurement Capabilities of Planar Doppler Velocimetry Using Pulsed Lasers," *Applied Optics*, Vol. 35, No. 6, 1996, pp. 948–964.

[16]McKenzie, R. L., "Planar Doppler Velocimetry Performance in Low-Speed Flows," AIAA Paper 97-0498, Jan. 1997.

[17]Beutner, T. J., Elliott, G. S., Mosedale, A. D., and Carter, C. D., "Doppler Global Velocimetry Applications in Large-Scale Facilities," AIAA Paper 98-2608, June 1998.

[18]Mosedale, A., Elliott, G. S., Carter, C. D., and Beutner, T. J., "On the Use of Planar Doppler Velocimetry," *AIAA Journal*, Vol. 38, No. 6, 2000, pp. 1010–1024.

[19]Mosedale, A., "An Investigation of the Planar Doppler Velocimetry Technique," M.S. Thesis, Dept. of Mechanical and Aerospace Engineering, Rutgers Univ., New Brunswick, NJ, Oct. 1998.

[20]Gogineni, S., Goss, L., Pestian, D., and Rivir, R., "Two-Color Digital PIV Employing a Single CCD Camera," *Experiments in Fluids*, Vol. 25, No. 4, 1998, pp. 320–328.

[21]Smith, M. W., "The Reduction of Laser Speckle Noise in Planar Doppler Velocimetry," AIAA Paper 98-2607, June 1998.

[22]Kerker, M., *The Scattering of Light and Other Electromagnetic Radiation*, Academic Press, San Diego, CA, 1969, pp. 27–74.

[23]Kerker, M., Scheiner, P., and Cooke, D. D., "The Range of Validity of the Rayleigh and Thomson Limits for Lorenz–Mie Scattering," *Journal of the Optical Society of America*, Vol. 68, No. 1, 1978, pp. 135–137.

[24]van de Hulst, H. C., *Light Scattering by Small Particles*, Dover, New York, 1981, pp. 114–171.

[25]Forkey, J. N., "Development and Demonstration of Filtered Rayleigh Scattering—A Laser-Based Flow Diagnostic for Planar Measurement of Velocity, Temperature, and Pressure," Final Rept. for NASA Graduate Student Research, Fellowship Grant NGT-50826, 1996.

[26]Forkey, J. N., Finkelstein, N. D., Lempert, W. R., and Miles, R. B., "Demonstration and Characterization of Filtered Rayleigh Scattering for Planar Velocity Measurements," *AIAA Journal*, Vol. 34, No. 3, 1996, pp. 442–448.

M. Samimy
Associate Editor

Color reproductions courtesy of Sverdrup Technology, Inc.